The (e, 2e) triple differential cross sections of Cu^+ (3p) in coplanar asymmetric geometry*

Zhou Li-Xia(周丽霞)†, Yan You-Guo(燕友果), and Men Fu-Dian(门福殿)

College of Physics Science and Technology, China University of Petroleum, Dongying 257061, *China*

(Received 5 May 2009; revised manuscript received 25 January 2010)

The three-body distorted-wave Born approximation has been used to calculate the (e, 2e) triple differential cross sections (TDCSs) of Cu^+ (3p) in different kinematical variables in coplanar asymmetric geometry. The angles 4°, 10° and 20° were selected as the scattering electron angles. Under high incident energy ($\geq$ 500 eV) and high asymmetric detection energy, the binary peaks showed abnormal splits. Such abnormal splits have not been observed in atomic target and outer valence orbitals of ionic target, which indicates that an (e, 2e) process for inner valence orbitals of ionic target would be more complicated than outer valence orbitals. Furthermore, some pronounced peaks appeared at certain ejected angles. We considered that these pronounced peaks are probably related to one kind of double-binary collision.

Keywords: (e, 2e), distorted-wave Born approximation, triple differential cross sections, double-binary collision

PACC: 3480D, 3450H

1. Introduction

The electron impact ionization of an atom or ion with coincidence detection of the three-particle final state, so-called an (e, 2e) reaction, provided detailed information of the ionization mechanism and dynamics of three charged particles moving in the three-body continuum. He, Ne, Ar, Kr, and Xe were familiar objects. The outer and inner valence (e, 2e) triple differential cross sections (TDCSs) of these targets have been extensively researched. In 1969, Ehrhardt *et al.*[1] reported the experimental and theoretical (e, 2e) TDCSs of He. The TDCSs showed two obvious peaks, which are well known as binary peak and recoil peak. In the process of collision, the orbital electrons were knocked out by incident electrons and formed the binary peak, which always appeared in the direction of momentum transfer $\boldsymbol{K}$. If the ejected electrons were recoiled by target ions, the recoil peak would emerge. Recoil peak always appeared in the opposite direction of momentum transfer $\boldsymbol{K}$. In the following decades, the binary and recoil peaks of other inert gas atoms were also extensively researched.[2−11] For s orbital, the binary and recoil peaks were often single. But for p orbital, the binary peaks probably split into two peaks.[3,10,11] Ehrhardt *et al.*[11] gave a reasonable explanation for the split of p orbital. They considered that the split could be ascribed to the electron momentum distributions of p orbital. The electron momentum profile of s orbital had a maximum value at electron momentum $p = 0$. But for p orbital, the electron momentum profile showed one peak in the region of $p > 0$ and gave minimum value at $p = 0$. Here, the peak position of p orbital was defined as $p_{\max}$ and the difference between ejected electron momentum k_2 and momentum transfer $\boldsymbol{K}$ as Δp. According to Ehrhardt *et al.*[11] if Δp was smaller than $p_{\max}$, the binary peak for p orbital would split into two peaks.

The (e, 2e) researches for ionic targets played an important role in the fields of astrophysics, plasma physics and fusion. However, due to the low density of ion sources, few experimental measurements of (e, 2e) reaction for ionic targets have been reported.[12] So, numerous theoretical studies have been carried out. Khajuria *et al.*[13,14] calculated the TDCSs of p orbital for alkali metal ions in different geometry using distorted-wave Born approximation (DWBA) and distorted-wave impulse approximation (DWIA) theory. Their research indicated that the ratio of binary-to-recoil peak depended on $\boldsymbol{K}$ for a fixed incident energy. In addition, they also found the split of binary peak under some dynamic conditions. Chen *et al.*[15] reported the (e, 2e) TDCSs of Li^+ ($2s^2$) and K^+ ($3p^6$) in coplanar asymmetric geometry, and found that the binary peak moved to angles higher than that of $\boldsymbol{K}$.

*Project supported by Shandong Provincial Natural Science Foundation of China (Grant No. Q2008A07).

†Corresponding author. E-mail: zhoulx@upc.edu.cn

© 2010 Chinese Physical Society and IOP Publishing Ltd

They used a double-binary encounter mechanism to explain such a phenomenon. An (e, 2e) research on hydrogen ions in coplanar asymmetric geometry has been reported by Shi *et al.*[16] Besides binary peaks and recoil peaks, a new peak appeared in forward direction (ejected angle less than 180°) when $Z \geq 4$ (Z denotes atomic number). They considered a double-binary encounter process has happened in the (e, 2e) reaction.

Though some (e, 2e) researches have been reported the outer shell p orbital for ionic targets, the research on inner shell p orbital of ionic targets has not been reported. In this paper, we first calculated the (e, 2e) TDCSs of inner shell 3p orbital for Cu^+ with different kinematical variables. At high incident energy ($\geq$ 500 eV) and highly asymmetric detection energy, an abnormal split of binary peak was observed, which has not been reported in TDCSs of atomic targets and outer valence orbitals of ionic targets. Furthermore, we found some pronounced peaks that appeared at certain angles. A double-binary collision process was proposed to explain the appearance of these new peaks.

2. Theory

Considering a Cu^+ ion ionized by impact of an incident electron with momentum k_0 followed by two electrons outgoing with momentum k_1 and k_2, the TDCS for such a process could be described by DWBA theory as[17]

$$\frac{\mathrm{d}^3\sigma^{\mathrm{DWBA}}}{\mathrm{d}\Omega_1\mathrm{d}\Omega_2\mathrm{d}E_1} = (2\pi)^4\frac{k_1k_2}{k_0}\sum_{\mathrm{av}}\left[|f|^2+|g|^2-\mathrm{Re}(f^*g)\right], \quad (1)$$

where

$$f = \left\langle \chi^{(-)}(k_1,r_1)\chi^{(-)}(k_2,r_2)\left|\frac{1}{r_{12}}\right|\chi^{(+)}(k_0,r_0)\psi_{nl}\right\rangle, \quad (2)$$

$$g = \left\langle \chi^{(-)}(k_1,r_2)\chi^{(-)}(k_2,r_1)\left|\frac{1}{r_{12}}\right|\chi^{(+)}(k_0,r_0)\psi_{nl}\right\rangle. \quad (3)$$

In the above equations, $\sum_{\mathrm{av}}$ represents the sum over final and average over initial magnetic and spin degeneracy; ψ_{nl} is the orbital of Cu^+, $\chi^{(+)}$ denotes the distorted wave of incident electron generated in the equivalent local ground state potential of Cu^+ ion, and $\chi^{(-)}$ is the distorted wave of outgoing electrons generated in the equivalent local ground state potential of ion in final channels; $\chi^{(+)}$ and $\chi^{(-)}$ are both orthogonal to ψ_{nl}.

The equivalent local ground state potential $V_{00}(r)$ (i.e. distorting potential) was the sum of direct potential V_{D} and exchange potential V_{E}. The direct potential V_{D} was obtained from the target-ion radial orbitals $u_{nl}(r)$.[17]

$$V_{\mathrm{D}}(r) = \sum_{nl} N_{nl}\int \mathrm{d}r'[u_{nl}(r')]^2/r_> , \quad (4)$$

where $r_>$ is the greater one of r and r', N_{nl} is the number of electrons in orbital nl. The spin average static exchange potential V_{E} is given by[18]

$$\begin{aligned} &V_{\mathrm{E}}(r) \\ &= 0.5\left\{E - V_{\mathrm{D}}(r) + \frac{3}{10}[3\pi^2\rho(r)]^{2/3}\right\} \\ &\quad - 0.5\Bigg\{[E - V_{\mathrm{D}}(r) + \frac{3}{10}[3\pi^2\rho(r)]^{2/3}]^2 \\ &\quad +4\pi\rho(r)\Bigg\}^{1/2}, \end{aligned} \quad (5)$$

where $\rho(r)$ is the electron density. And then, the equivalent distorting potential $V_{00}(r)$ could be described as

$$V_{00}(r) = V_{\mathrm{D}}(r) + V_{\mathrm{E}}(r). \quad (6)$$

3. Results and discussions

Figure 1 shows the TDCSs of electron impact ionization of $Cu^+(3p)$ with ejected electron energy $E_2 = 10$ eV in coplanar asymmetry geometry. Figures 1(a)–1(d) represent the TDCSs at incident energy $E_0 = 1000$, 500, 200 and 150 eV, respectively. The detected angles of scattering electron are fixed at $\theta_1 = 4°$, 10° and 20°, and the corresponding TDCSs are denoted by solid, dashed and dot-dashed lines in Figs. 1(a)–1(d). $\boldsymbol{K}$ and Δp are shown in Table 1.

At incident energy 1000 eV (Fig. 1(a)), when the scattering electron angle is $\theta_1 = 4°$, the binary peak splits into two peaks, while the recoil peak does not. When $\theta_1 = 10°$, both the binary peak and recoil peak do not split. When $\theta_1 = 20°$, both peaks split into two peaks.

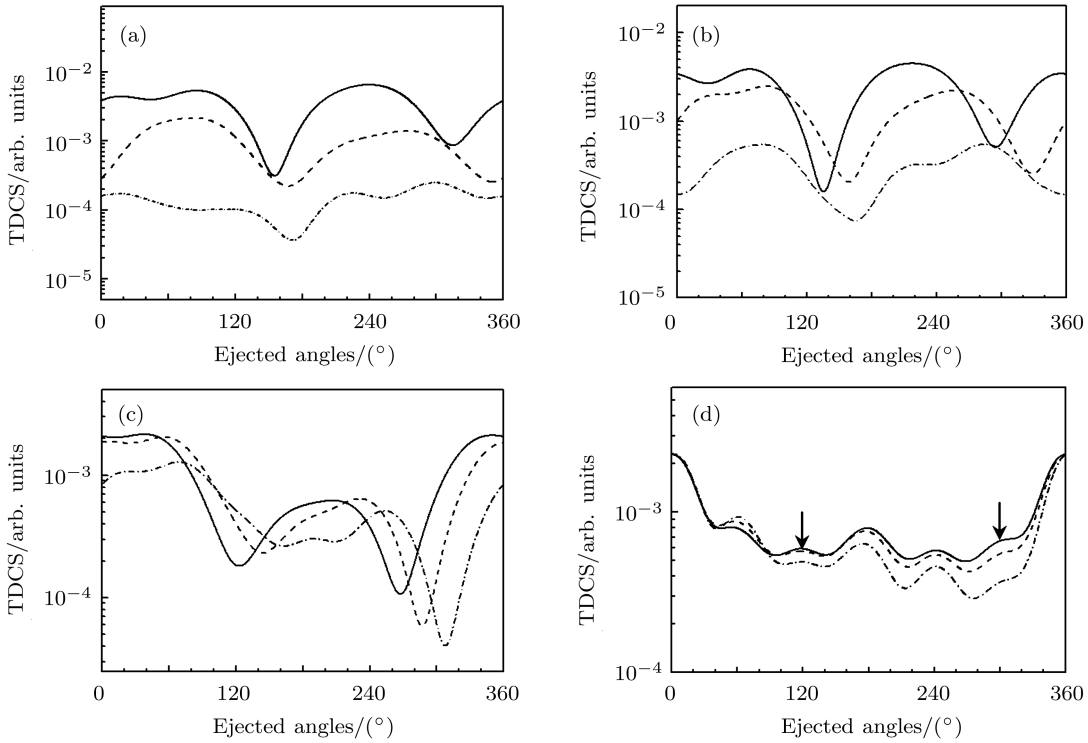


Fig. 1. TDCSs of electron impact ionization of $Cu^+(3p)$ with ejected electron energy $E_2 = 10$ eV in coplanar asymmetric geometry: (a) incident energy $E_0 = 1000$ eV, (b) incident energy $E_0 = 500$ eV, (c) incident energy $E_0 = 200$ eV, and (d) incident energy $E_0 = 150$ eV. The TDCSs at $\theta_1 = 4°$, 10° and 20° are denoted by solid, dash and dot-dashed lines, respectively.

Table 1. Momentum transfer $\boldsymbol{K}$ and Δp, where Δp denotes the absolute value of difference between $\boldsymbol{K}$ and ejected electron momentum k_2. The energy of the ejected electron is 10 eV.

E_0/eV	θ_1/(°)	$\boldsymbol{K}$/arb. units	Δp/arb. units
1000	4	0.75	2.06
1000	10	1.53	1.28
1000	20	2.93	0.12
500	4	0.79	1.86
500	10	1.21	1.60
500	20	2.10	0.71
200	4	1.24	1.57
200	10	1.34	1.47
200	20	1.64	1.17
150	4	1.55	1.26
150	10	1.60	1.21
150	20	1.75	1.06

Further, we calculate the electron momentum profile for 3p orbital of Cu^+ using density functional theory DFT–B3LYP with Lanl2dz basis set. The results are shown in Fig. 2. It can be seen that $p_{\max}$ is about 1.61 a.u.. Compared with the Δp(as shown in Table 1), at $\theta_1 = 4°$, $\Delta p > p_{\max}$, whereas, at $\theta_1 = 10°$ and 20°, $\Delta p < p_{\max}$. According to Ehrhardt *et al.*,[11] if $\Delta p < p_{\max}$, the binary peak in (e, 2e) TDCSs will split into two peaks, otherwise, it would not split.

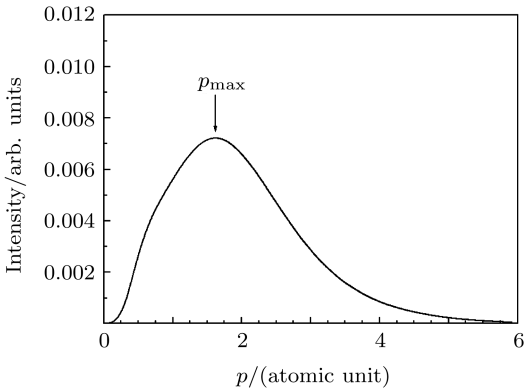


Fig. 2. Electron momentum distribution of $Cu^+(3p)$ calculated using density functional theory DFT-B3LYP with Lanl2dz basis set.

Based on the above theory, the binary peak will split into two peaks at $\theta_1 = 10°$ and 20°, but not split at $\theta_1 = 4°$. However, our calculated results (Fig. 1(a)) are abnormal results, i.e., the binary peak splits into two peaks at $\theta_1 = 4°$ but not split at $\theta_1 = 10°$. Such

an abnormal split for p orbital has never been reported for atomic targets and the outer valence orbitals of ionic targets, indicating that the (e, 2e) process for inner valence orbital of ionic targets might be more complicated.

We further calculate the TDCSs at incident energies 500, 200, and 150 eV with ejected electron energies fixed at 10 eV (see Figs. 1(b)–1(d)), the corresponding Δp are also calculated and shown in Table 1.

In Fig. 1(b), at $\theta_1 = 4°$, $\Delta p > p_{\max}$, the binary peak should not split, while the peak splits in our calculated results. At $\theta_1 = 10°$, $\Delta p < p_{\max}$, the binary peaks should split into two peaks, and the binary peaks of the TDCSs indeed split in our calculated results. At $\theta_1 = 20°$, $\Delta p < p_{\max}$, the binary peak should split, while the peak does not split in our calculated results. So, the binary peak split abnormally at $\theta_1 = 4°$ and 20°.

In Figs. 1(c) and 1(d), at $\theta_1 = 4°$, 10° and 20°, the Δp are all less than $p_{\max}$, the binary peaks should split into two peaks, and the binary peaks of the TDCSs indeed split in our calculated results.

In Fig. 1(d), it is worth noting that two new peaks emerge at ejected angle $\theta_2 \sim 120°$ and $\theta_2 \sim 300°$ (indicated by arrows), which means some double-binary collisions.[19] The probable double-binary collisions are shown in Fig. 3, where 3(a) and 3(b) show that the incident electron first interacts with orbital electron being knocked out as e_2. The scattering electron (e_1) is scattered elastically off the nucleus again, and steered to a direction at angle θ_1. In Figs. 3(c) and 3(d), the incident electron is first scattered elastically off the nucleus, and then collides with the orbital electron, and subsequently emerges at angle θ_1.

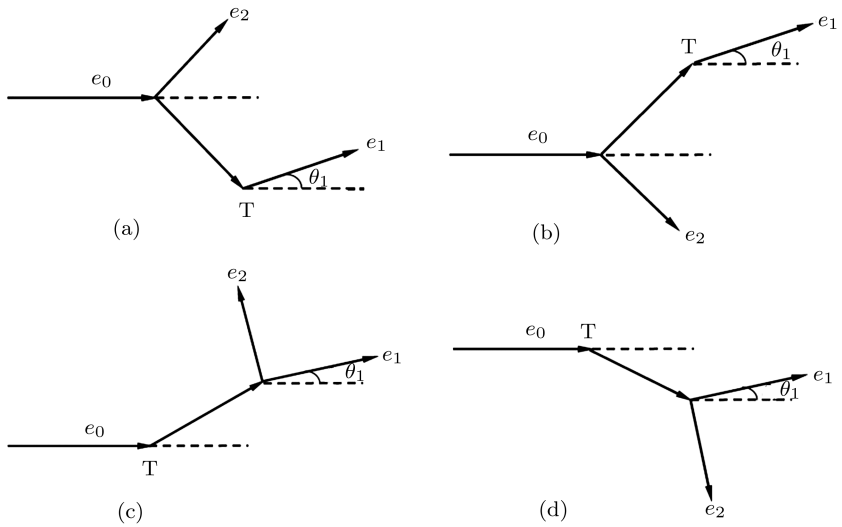


Fig. 3. Various double-binary collision processes, T denotes the target nucleus.

In Figs. 3(a) and 3(b), the ejected electron (e_2) emerges in the ranges of $0 < \theta_2 < 90°$ and $270° < \theta_2 < 360°$. In Fig. 3(c) and 3(d), the ejected electron emerges in the ranges $90° < \theta_2 < 180°$ (the ejected electron direction in this region is regarded as forward direction) and $270° < \theta_2 < 360°$ (the ejected electron direction in this region is regarded as backward direction).

Based on the angle range of the ejected electron in Fig. 3, it can be concluded that the new peak at $\theta_2 \sim 120°$ in Fig. 1(d) can be attributed to the colliding process in Fig. 3(c). The other new peak at $\theta_2 \sim 300°$ in Fig. 1(d) can be attributed to the colliding process in Figs. 3(b) or 3(d).

The (e, 2e) process satisfies the energy conservation condition, and the angle between ejected electron and incident electron or the angle between scattering electron and incident electron in (e, 2e) reaction can be calculated. The sum of these two angles is the angle between the directions of ejected electron and scattering electron, which equals 90°. In addition, the ejected electron angles may change with different incident energy and outgoing electron energy for the same angle of detected scattering electron in Fig. 3(b), while they

will not change in Figs. 3(c) and 3(d).

We further calculate the TDCSs of Cu^+ (3p) of the scattering electron and ejected electron with different energy. The scattering electron energy E_1 and ejected electron energy E_2 are set to (93, 30), (93, 60), (243, 160), and (203, 200). The calculated TDCSs of above four energy sets are shown in Figs. 4(a)–4(d). The solid, dashed, and dot-dashed lines represent the TDCSs for scattering angles 4°, 10°, and 20°, respectively.

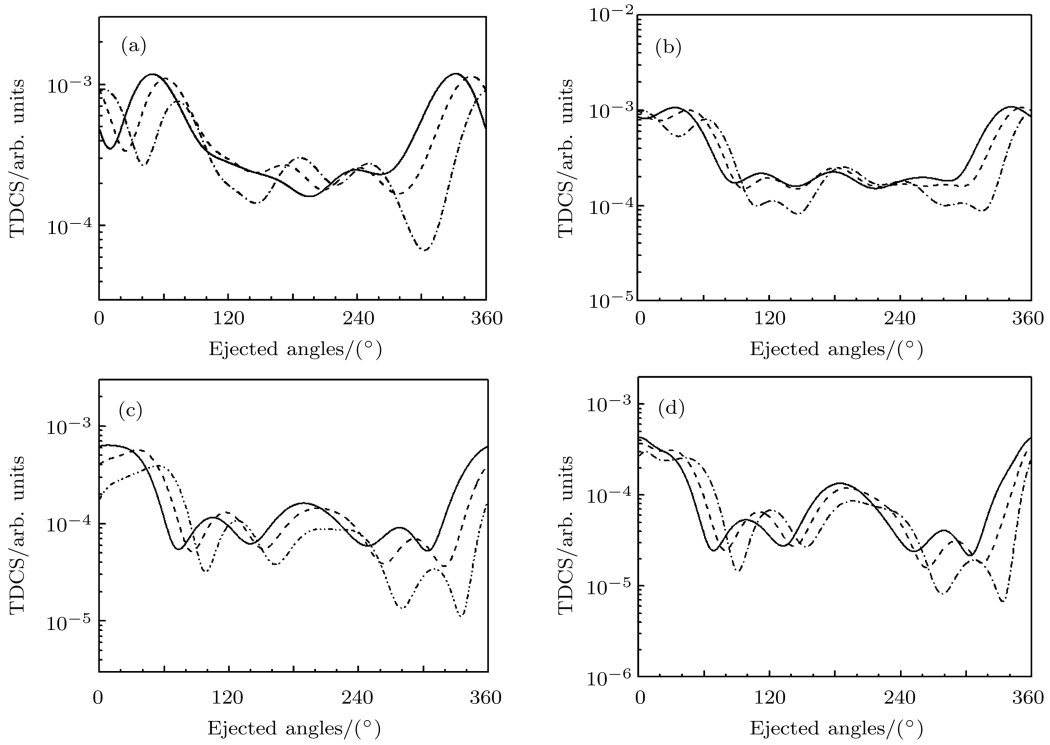


Fig. 4. TDCSs for electron impact ionization of Cu^+(3p) in coplanar asymmetric geometry. Scattering electron energy E_1 and ejected electron energy E_2 are (a) (93, 30), (b) (93, 60), (c) (243, 160), and (d) (203, 200). The TDCSs at $\theta_1 = 4°$, 10° and 20° are represented by solid, dashed, and dot-dashed lines, respectively.

From Fig. 4, it can be seen that all TDCSs show two obvious double-binary collision peaks except for a small shoulder at $\theta_2 \sim 120°$ in Fig. 4(a). The position of the double-binary collision peaks for different E_1, E_2, and scattering angles are given in Table 2. From Table 2, for the same scattering angle θ_1 and different E_1 and E_2, the change of θ_{21} or θ_{22} is small. The θ_{21} and θ_{22} are about 120° and 300°, respectively, which is in agreement with the processes described in Figs. 3(c) and 3(d). It is worth noting that there is still a little difference between these calculated results and our evaluation. Based on the explanation of Brauner *et al.*,[19] the difference may come from the interaction between scattering electron and ejected electron.

Table 2. Position of double-binary collision peaks. The angles θ_{21} and θ_{22} denote the ejected angles of the forward peak and backward peak, respectively.

E_1/eV	E_2/eV	θ_1/(°)	θ_{21}/(°)	θ_{22}/(°)
43[a]	10	4	120	300
43[a]	10	10	120	300
43[a]	10	20	120	300
93	30	4	–	–
93	30	10	–	–
93	30	20	–	–
93	60	4	115	260
93	60	10	120	280
93	60	20	125	295
243	160	4	105	280
243	160	10	115	290
243	160	20	130	310
203	200	4	100	280
203	200	10	110	290
203	200	20	120	305

[a] incident energy: 150 eV.

4. Conclusion

The TDCSs of Cu^+ (3p) have been calculated using the three-body distorted-wave Born approximation with different kinematical variables in coplanar asymmetric geometry at scattering electron angles $\theta_1 = 4°$, $10°$ and $20°$. We found an abnormal split when incident electron energy was 1000 eV or 500 eV and in high asymmetric detection energy, which have not been reported for atomic targets and outer valence orbitals of ionic targets. This phenomenon indicated that the (e, 2e) process for inner valence orbitals of ionic targets may be more complicated. In addition, we found some pronounced peaks appearing at certain ejected angles when the difference between ejected electron energy and scattering electron energy was small. These peaks were attributed to one kind of double-binary collision.

References

[1] Ehrhardt H, Schulz M, Tekaat T and Willmann K 1969 *Phys. Rev. Lett.* **22** 89

[2] Staicu-Casagrande E M, Catoire F, Naja A, Ren X G, Lahmam-Bennani A, Nekkab M, Cappello C D, Bartschat K and Whelan C T 2007 *J. Electron. Spectrosc. Rel. Phenom.* **161** 27

[3] Wu X J, Chen X J, Shan X, Chen L Q and Xu K Z 2004 *Chin. Phys.* **13** 1857

[4] Zhou L X and Yan Y G 2008 *Acta Phys. Sin.* **57** 7619 (in Chinese)

[5] Yang H, Gao K and Zhang S M 2007 *Acta Phys. Sin.* **56** 5202 (in Chinese)

[6] Murray A J and Read F H 2000 *Phys. Rev.* A **63** 012714

[7] Haynes M A, Lohmann B, Prideaux A and Madison D H 2003 *J. Phys.* B: *At. Mol. Opt. Phys.* **36** 811

[8] Zhang S M, Chen Z J and Xu K Z 1999 *Acta Phys. Sin.* **48** 453 (in Chinese)

[9] Zhang S M, Chen Z J, Shi Q C and Xu K Z 1997 *Acta Phys. Sin.* **46** 2320 (in Chinese)

[10] Avaldi L, Camilloni R, Multari R, Stefani G, Zhang X, Walters H R J and Whelan C T 1993 *Phys. Rev.* A **48** 1195

[11] Ehrhardt H, Hesselbacher K H, Jung K, Schubert E and Willmann K 1974 *J. Phys.* B: *At. Mol. Opt. Phys.* **7** 69

[12] Bolognesi P, Pravica L, Veronesi S, Fainelli E, Avaldi L and Bartschat K 2008 *J. Phys.* B: *At. Mol. Opt. Phys.* **41** 065203

[13] Khajuria Y, Chen L Q, Chen X J and Xu K Z 2002 *J. Phys.* B: *At. Mol. Opt. Phys.* **35** 93

[14] Khajuria Y and Tripathi D N 1999 *Phys. Rev.* A **59** 1197

[15] Chen L Q, Chen X J, Wu X J, Shan X and Xu K Z 2005 *J. Phys.* B: *At. Mol. Opt. Phys.* **38** 1371

[16] Shi Q C, Chen Z J, Chen J and Xu K Z 1997 *J. Phys.* B: *At. Mol. Opt. Phys.* **30** 2859

[17] McCarthy I E 1995 *Aust. J. Phys.* **48** 1

[18] Gianturco F A and Scialla S 1987 *J. Phys.* B: *At. Mol. Phys.* **20** 3171

[19] Brauner M and Briggs J S 1993 *J. Phys.* B: *At. Mol. Phys.* **26** 2451